

Northern Hemisphere atmospheric influence of the solar proton events and ground level enhancement in January 2005

C. H. Jackman¹, D. R. Marsh², F. M. Vitt², R. G. Roble², C. E. Randall³, P. F. Bernath⁴, B. Funke⁵, M. López-Puertas⁵, S. Versick⁶, G. P. Stiller⁶, A. J. Tylka⁷, and E. L. Fleming^{1,8}

¹NASA Goddard Space Flight Center, Greenbelt, Maryland, USA

²National Center for Atmospheric Research, Boulder, Colorado, USA

³University of Colorado, Boulder, Colorado, USA

⁴University of York, York, UK

⁵Instituto de Astrofísica de Andalucía, CSIC, Granada, Spain

⁶Karlsruhe Institute of Technology, Karlsruhe, Germany

⁷Naval Research Laboratory, Washington, DC, USA

⁸Science Systems and Applications Inc., Lanham, Maryland, USA

Received: 6 January 2011 – Published in Atmos. Chem. Phys. Discuss.: 7 March 2011

Revised: 13 June 2011 – Accepted: 17 June 2011 – Published: 1 July 2011

Abstract. Solar eruptions in early 2005 led to a substantial barrage of charged particles on the Earth's atmosphere during the 16–21 January period. Proton fluxes were greatly increased during these several days and led to the production of HO_x (H, OH, HO₂) and NO_x (N, NO, NO₂), which then caused the destruction of ozone. We focus on the Northern polar region, where satellite measurements and simulations with the Whole Atmosphere Community Climate Model (WACCM3) showed large enhancements in mesospheric HO_x and NO_x constituents, and associated ozone reductions, due to these solar proton events (SPEs). The WACCM3 simulations show enhanced short-lived OH and HO₂ concentrations throughout the mesosphere in the 60–82.5° N latitude band due to the SPEs for most days in the 16–21 January 2005 period, somewhat higher in abundance than those observed by the Aura Microwave Limb Sounder (MLS). These HO_x enhancements led to huge predicted and MLS-measured ozone decreases of greater than 40 % throughout most of the northern polar mesosphere during the SPE period. Envisat Michelson Interferometer for Passive Atmospheric Sounding (MIPAS) measurements of hydrogen peroxide (H₂O₂) show increases throughout the stratosphere with highest enhancements of about 60 pptv in the lowermost mesosphere over the 16–18 January 2005 period due to the solar protons. WACCM3 predictions indicate H₂O₂ enhancements over the same time period of about three

times that amount. Measurements of nitric acid (HNO₃) by both MLS and MIPAS show an increase of about 1 ppbv above background levels in the upper stratosphere during 16–29 January 2005. WACCM3 simulations show only minuscule HNO₃ increases (< 0.05 ppbv) in the upper stratosphere during this time period. Polar mesospheric enhancements of NO_x are computed to be greater than 50 ppbv during the SPE period due to the small loss rates during winter. Computed NO_x increases, which were statistically significant at the 95 % level, lasted about a month past the SPEs. The SCISAT-1 Atmospheric Chemistry Experiment Fourier Transform Spectrometer NO_x measurements and MIPAS NO₂ measurements for the polar Northern Hemisphere are in reasonable agreement with these predictions. An extremely large ground level enhancement (GLE) occurred during the SPE period on 20 January 2005. We find that protons of energies 300 to 20 000 MeV, associated with this GLE, led to very small enhanced lower stratospheric odd nitrogen concentrations of less than 0.1 % and ozone decreases of less than 0.01 %.

1 Introduction

Large solar eruptions during 16–21 January 2005 caused huge fluxes of high-energy solar charged particles to reach Earth. The solar proton flux enhancement during this period has been well documented and caused significant production of OH (Verronen et al., 2006; Damiani et al., 2008) and destruction of ozone (Verronen et al., 2006; Seppälä et al.,



Correspondence to: C. H. Jackman
(charles.h.jackman@nasa.gov)

2006; Klekociuk et al., 2007; Damiani et al., 2008). The largest ground level enhancement (GLE) of neutrons during solar cycle 23 also occurred in this period. A neutron monitor registered an increase of about 270 % on 20 January 2005 during the GLE (Gopalswamy et al., 2005).

We recently studied the short- and medium-term (days to a few months) atmospheric constituent effects of the four largest solar proton events (SPEs) in the past 45 years (August 1972, October 1989, July 2000, and October–November 2003) in Jackman et al. (2008) with version 3 of the Whole Atmosphere Community Climate Model (WACCM3). The present investigation builds on that study and focuses on the short- and medium-term influences of solar particles on the mesosphere and stratosphere in the time period 1 January through 31 March 2005. There was substantial solar activity in January 2005, which was also the period of the eleventh largest SPE period in the past 45 years (Jackman et al., 2008). We include SPEs in January 2005 and the highest energy protons leading to the GLE on 20 January 2005 in our WACCM3 computations. Larger and longer-lasting impacts were expected in the northern winter polar region because of the diminished sunlight and general downward transport. We, therefore, focus on the impact of the solar particles on constituents in the northern polar mesosphere and stratosphere. The highly energetic solar particles produced HO_x (H, OH, HO_2) and NO_x (N, NO, NO_2), which then led to ozone variations. We compare the WACCM3 predictions during this period with measurements from three platforms: Aura Microwave Limb Sounder (MLS) of OH, HO_2 , HNO_3 , and ozone; Envisat Michelson Interferometer for Passive Atmospheric Sounding (MIPAS) of H_2O_2 , NO_2 , and HNO_3 ; and SCISAT-1 Atmospheric Chemistry Experiment Fourier Transform Spectrometer (ACE-FTS) of NO and NO_2 .

This paper is divided into seven sections, including the Introduction. The charged particle flux and ionization rate are discussed in Sect. 2. HO_x and NO_x production are discussed in Sect. 3. A description of WACCM3 is given in Sect. 4. The modeled and measured influences of the January 2005 SPEs over the 1 January–31 March 2005 period are shown in Sect. 5. The influence of the 20 January 2005 GLE is shown in Sect. 6 and the conclusions are presented in Sect. 7.

2 Charged particle flux and ionization rate

Our WACCM3 computations with charged particle flux included: (1) the solar proton flux (energies 1 to 300 MeV) over the 1 January–31 March 2005 period; and (2) the highest energy protons (300 to 20 000 MeV) associated with a GLE of neutrons on 20 January 2005. We performed separate WACCM3 simulations with no charged particle flux, charged particles described in (1), and charged particles described in both (1) and (2). These model simulations are described in Sect. 4.

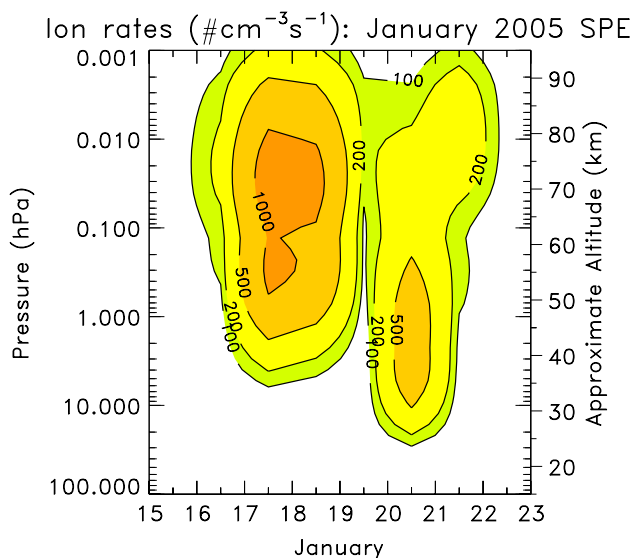


Fig. 1. Daily average ion pair production rates ($\# \text{cm}^{-3} \text{s}^{-1}$) for the “SPEs-only” case (protons with energy 1–300 MeV) as a function of time for 15–22 January 2005.

The solar proton flux (energies 1 to 300 MeV) for 2005 was provided by the National Oceanic and Atmospheric Administration (NOAA) Geostationary Operational Environmental Satellite, GOES-11 (Jackman et al., 2008). The proton flux data from the satellite were used to compute ion pair production profiles using the energy deposition methodology discussed in Jackman et al. (1980), where the creation of one ion pair was assumed to require 35 eV (Porter et al., 1976). The SPE-produced daily average ionization rates are given in Fig. 1 for the eight day period, 15–22 January 2005, from 100 hPa (~ 16 km) to 0.001 hPa (~ 96 km). There were two periods of SPEs in these eight days, 16–18 January and 20–21 January. The first period was the most intense with peak ionization above $1000 \text{ cm}^{-3} \text{ s}^{-1}$ for the 0.01 to 1 hPa region. The second period showed peak ionization above $500 \text{ cm}^{-3} \text{ s}^{-1}$ for the 0.2 to 10 hPa region.

We included the highest energy protons (300 to 20 000 MeV) associated with the GLE of neutrons on 20 January 2005 in some computations with “SPEs + GLE”. This high energy proton flux was taken from the spectrum given in Usoskin et al. (2009, 2011), which was derived using methodology presented in Tytko and Dietrich (2009). The calculated GLE ionization rate on 20 January 2005 was added to the computed ionization rate from the GOES-11 measured protons for some of the model computations (see Sect. 4). Ionization rates on 20 January 2005 between 10 and 100 hPa for “SPEs-only” and “SPEs + GLE” are compared in Fig. 2. At 10 hPa the ionization is primarily caused by the SPEs; ionization caused by the GLE rapidly increases in importance below 10 hPa, and is more than an order of magnitude larger than ionization by the SPEs at 40 hPa.

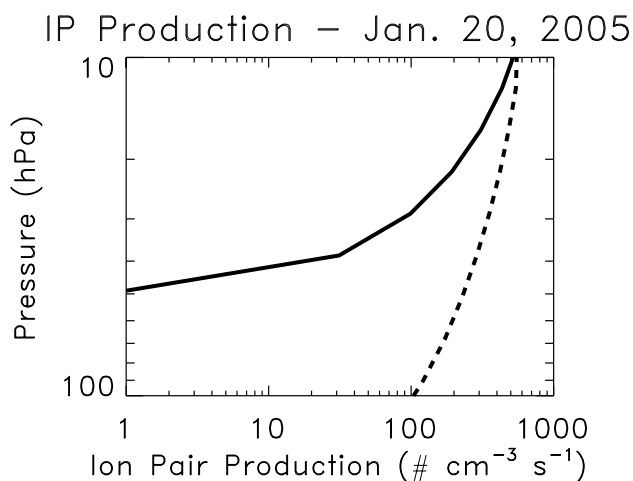


Fig. 2. Daily average ion pair production rates ($\text{cm}^{-3} \text{s}^{-1}$) computed for the “SPEs-only” case (solid line) and the “SPEs + GLE” case (dashed line) on 20 January 2005.

Table 1. Description of WACCM3 simulations.

Simulation designation	Number of realizations	Time period	SPEs included	GLE included
A (1, 2, 3, 4)	4	1 Jan–31 Mar 2005	No	No
B (1, 2, 3, 4)	4	1 Jan–31 Mar 2005	Yes	No
C (1, 2, 3, 4)	4	1 Jan–31 Mar 2005	Yes	Yes

3 HO_x and NO_x production

Charged particle precipitation results in the production of HO_x through complex positive ion chemistry (Solomon et al., 1981). The charged particle-produced HO_x is a function of ion pair production and altitude and is included in WACCM3 simulations using a lookup table from Jackman et al. (2005a, Table 1), which is based on the work of Solomon et al. (1981). Verronen et al. (2006) have noted that HNO₃ is produced along with the HO_x, ultimately leading to a delayed production of HO_x. Currently, WACCM3 does not include this production of HNO₃ and only includes the HO_x production. Even though the HO_x constituents have a relatively short lifetime (\sim hours) throughout most of the mesosphere, the ozone depletion can be very large during substantial SPEs (e.g., Solomon et al., 1983; Jackman et al., 2001; Verronen et al., 2006). This HO_x-induced ozone depletion can have an influence on the mesospheric temperature and winds over a relatively short period of time (\sim 4–6 weeks), see Jackman et al. (2007).

NO_x is produced when the energetic charged particles (protons and associated secondary electrons) dissociate N₂ as they precipitate into the atmosphere. Here we assume that \sim 1.25 N atoms are produced per ion pair and divide the proton impact of N atom production between ground state

N(⁴S) (\sim 45 % or \sim 0.55 per ion pair) and excited state N(²D) (\sim 55 % or \sim 0.7 per ion pair) nitrogen atoms (Porter et al., 1976). The N atoms react rapidly with other atmospheric constituents to form NO and, subsequently, NO₂.

4 Description of the whole atmosphere community climate model (WACCM3)

WACCM3 has been used in several previous studies to investigate the impact of natural and anthropogenic influences on the atmosphere from the troposphere through the middle atmosphere to the lower thermosphere (Sassi et al., 2002, 2004; Forkman et al., 2003; Richter and Garcia, 2006; Kinnison et al., 2007; Garcia et al., 2007; Marsh et al., 2007; Jackman et al., 2008, 2009). The model domain is from the surface to 4.5×10^{-6} hPa (about 145 km), with 66 vertical levels, and includes fully interactive dynamics, radiation, and chemistry. WACCM3 is based on the Community Atmosphere Model (CAM3) and includes modules from the Thermosphere-Ionosphere-Mesosphere-Electrodynamics General Circulation Model (TIME-GCM) and the Model for Ozone And Related chemical Tracers (MOZART-3) to simulate the dynamics and chemistry of the Earth’s atmosphere. The vertical resolution is \leq 1.5 km between the surface and about 25 km and increases slowly above 25 km to 2 km at the stratopause; it is 3.5 km in the mesosphere and one half the local scale height above the mesopause. The version of WACCM3 used here has latitude and longitude grid spacing of 4° and 5°, respectively. An extensive description of WACCM3 is given in Garcia et al. (2007) and Kinnison et al. (2007).

WACCM3 was forced in all simulations with observed time-dependent sea surface temperatures (SSTs), observed solar spectral irradiance and geomagnetic activity changes, and observed concentrations of greenhouse gases and halogen species over the simulation period (see Garcia et al., 2007). The geomagnetic activity included in all the WACCM3 simulations accounts for auroral precipitation, along with HO_x and NO_x production. However, these auroral particles mostly deposit their energy in the lower thermosphere (Marsh et al., 2007), whereas SPEs deposit most of their energy in the mesosphere and upper stratosphere. Medium energy electrons (MEEs) also impacted the atmosphere in January 2005. We have started work on including MEEs in future WACCM3 computations, however, the incorporation of MEEs is beyond the scope of the present study.

We have completed three 4-member ensemble WACCM3 simulations (described below) over the 1 January–31 March 2005 period: (A) four realizations [A(1, 2, 3, 4)] without any daily ionization rates from SPEs or the GLE; (B) four realizations [B(1, 2, 3, 4)] with the daily ionization rates from SPEs throughout the period; and (C) four realizations [C(1, 2, 3, 4)] with the daily ionization rates from SPEs throughout

the period and the GLE on 20 January. These WACCM3 simulations are summarized in Table 1.

The ionization rates, when included, were applied uniformly over both polar cap regions (60–90° N and 60–90° S geomagnetic latitude) as solar protons are guided by the Earth's magnetic field lines to approximately these areas (McPeters et al., 1981; Jackman et al., 2005a). Verronen et al. (2007) show that the geomagnetic boundary can vary with the proton forcing ranging from none to a full affect between about 57 and 64° N for the January 2005 SPEs time period. Our assumption of a uniform forcing over the entire polar cap may slightly overestimate the affected area. It does appear from the Verronen et al. study that the proton forcing is nearly a full effect at geomagnetic latitudes greater than about 62–63° N. If the affected polar cap is 62–90° N, rather than 60–90° N, then the impacted area would be decreased by about 13 %. Given that the proton flux's impacted region is variable with time and sometimes extends to latitudes lower than 60° geomagnetic, we have assumed a non-changing polar cap area for ease of computation. Due to the differing offsets of the geomagnetic and geographic poles in the two hemispheres, the effects from the SPEs and GLE are not expected to be symmetric in the Northern and Southern Hemispheres.

WACCM3 is a free-running GCM and the realizations' starting conditions were each slightly different from the other, initiated in January 1950. For all ensemble members WACCM3 was run in its free-running mode with identical boundary conditions from January 1950 up to 1 January 2005 (Garcia et al., 2007; Jackman et al., 2009), which is the starting date for all model computations shown in this paper. Simulations A1, B1, and C1 have the same starting conditions, except simulation A1 has “no SPEs and no GLE”, simulation B1 has “SPEs-only”, simulation C1 has “SPEs + GLE”. Similar comments apply to grouped simulations A2, B2, and C2; A3, B3, and C3; and A4, B4, and C4.

The WACCM3 daily average constituent computations are shown in comparison with measurements in this study.

5 Influences of the January 2005 SPEs

The mesosphere was perturbed by the SPEs in January 2005 as seen in the measurements of several satellite instruments and WACCM3 simulations. The short- (~ days) as well as medium- (~ weeks) term changes due to these solar influences will be discussed in this section.

5.1 Short-term influences

Since HO_x constituents have such short lifetimes (e.g., Solomon et al., 1981), a large enhancement of HO_x caused by an influx of protons during an SPE will be relatively short-lived (~ days). MLS provided measurements of two HO_x constituents, OH and HO₂ (Pickett et al., 2008). Previous pa-

pers have shown substantial HO_x and ozone impacts during the January 2005 SPEs (Verronen et al., 2006, 2007; Seppälä et al., 2006; Klekociuk et al., 2007; Damiani et al., 2008, 2009, 2010). We focus on the northern polar latitudes, a geographic region where HO_x constituents are at very small values in January due to minimal or no sunlight. The HO_x constituents in the winter polar region are, therefore, especially sensitive to solar proton impact in the mesosphere.

5.1.1 Hydroxyl radical (OH)

The Aura MLS OH measured enhancements due to the SPEs at 0.022 hPa for the Northern Hemisphere are given in Fig. 3 and were computed by subtracting the observations on 15 January 2005 (before the SPE) from the observations on 18 January 2005 (during the SPE). For added clarity, measurements are only shown northward of 42.5° N, however, no MLS measurements are available in the band 82.5–90° N. MLS measurements were binned into 30° longitude and 5° latitude bands. The polar cap edge (60° N geomagnetic latitude), wherein the protons are predicted to interact with the atmosphere, is indicated by the white circle. The MLS data shows that the SPE increased OH significantly: values greater than 4 ppbv are observed in a substantial part of the area poleward of 60° N geomagnetic latitude.

The WACCM3 OH predicted enhancements due to the SPEs at 0.022 hPa for the Northern Hemisphere are given in Fig. 4 and were computed from an average of the B realizations. In particular, the WACCM3 B average results on 15 January 2005 (before the SPE) were subtracted from the WACCM3 B results on 18 January 2005 (during the SPE). The MLS averaging kernel (AK) was also applied to the plotted WACCM3 results. For added clarity, the simulation results are only shown from 44–90° N. As in Fig. 3, the polar cap edge (60° geomagnetic latitude) is indicated by the white circle. WACCM3 also predicted a significant increase in OH: values greater than 4 ppbv are modeled in a substantial part of the area poleward of 60° N geomagnetic latitude. Both the MLS measurements and WACCM3 predictions indicate similar areas of enhanced OH as a result of the SPEs. The WACCM3 predictions do indicate a somewhat larger amount of OH change, when compared with MLS observations.

We compare the MLS OH measurements and WACCM3 model predictions for 16–23 January 2005 in the latitude band 60–82.5° N in Fig. 5. The first two weeks of January 2005 were relatively quiet and contained no SPEs. We thus used these first two weeks (1–14 January) to construct an average quiescent OH profile for both MLS and WACCM3, respectively. This respective quiescent OH profile was subtracted from the OH observations or predictions for 16–23 January 2005 and the results are given in Fig. 5. An average of the WACCM3 B realizations was used for this figure. As in Fig. 4, the MLS AK was applied to the plotted WACCM3 results.

OH (ppbv): 0.022 hPa – (Jan. 18 minus Jan. 15) – MLS

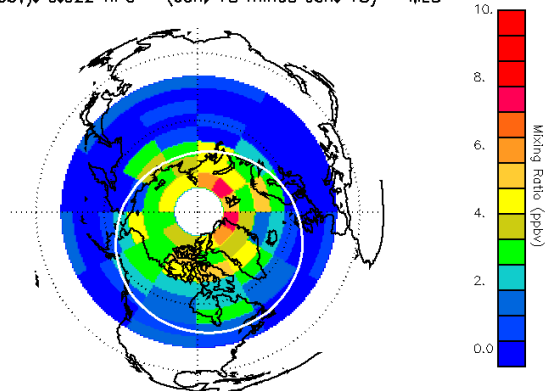


Fig. 3. Aura MLS OH measurements at 0.022 hPa (~ 75 km) on 18 January 2005 (after SPE) minus those on 15 January 2005 (before SPE). For added clarity, measurements are only shown in the latitude range 42.5 – 82.5° N. No MLS measurements are available at 82.5 – 90° N. The polar cap edge (60° geomagnetic latitude) is indicated by the white circle.

Fairly substantial OH enhancements are shown in the MLS measurements (up to 4 ppbv) and WACCM3 predictions (up to 6 ppbv) for the 16–23 January period. The OH increases were largest on 17–18 January, similar to the WACCM3 predictions. Similar to the comparisons between Figs. 3 and 4, the WACCM3 predictions of Fig. 5 do indicate a somewhat larger peak OH change, when compared with MLS observations.

5.1.2 Hydrogen dioxide (HO_2)

The MLS instrument additionally provides HO_2 measurements during the January 2005 period. Such measurements are somewhat noisier than the OH observations, however, MLS HO_2 does indicate enhancements above background levels (>0.1 ppbv) due to the January 2005 SPEs. Similar to Fig. 5, Fig. 6 was produced by averaging the HO_2 measurements over the quiet (non-SPE) period 1–14 January 2005 and subtracting this average from the HO_2 observations or predictions during 16–23 January 2005. Again, an average of the WACCM3 B realizations sampled with the MLS AK was used for Fig. 6.

As with OH, the WACCM3 predictions indicate a similar time frame for the HO_2 atmospheric perturbation when compared with MLS observations. Also, a somewhat larger HO_2 change is predicted than measured in the 16–21 January 2005 time period. The cause of the modeled/measured SPE-caused OH and HO_2 differences is not clear, but may be related to problems in the modeled representation of HO_x chemistry (Canty et al., 2006).

OH (ppbv): 0.022 hPa (Jan. 18 minus Jan. 15) – WACCM (B)

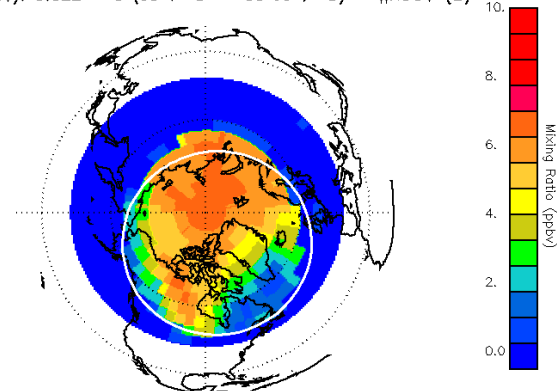


Fig. 4. WACCM3 B average OH predictions at 0.022 hPa (~ 75 km) on 18 January 2005 (after SPE) minus those on 15 January 2005 (before SPE). For added clarity, the results from the WACCM3 simulations are only shown from 44 – 90° N. The MLS averaging kernel (AK) was used to sample the WACCM3 results. The polar cap edge (60° geomagnetic latitude) is indicated by the white circle.

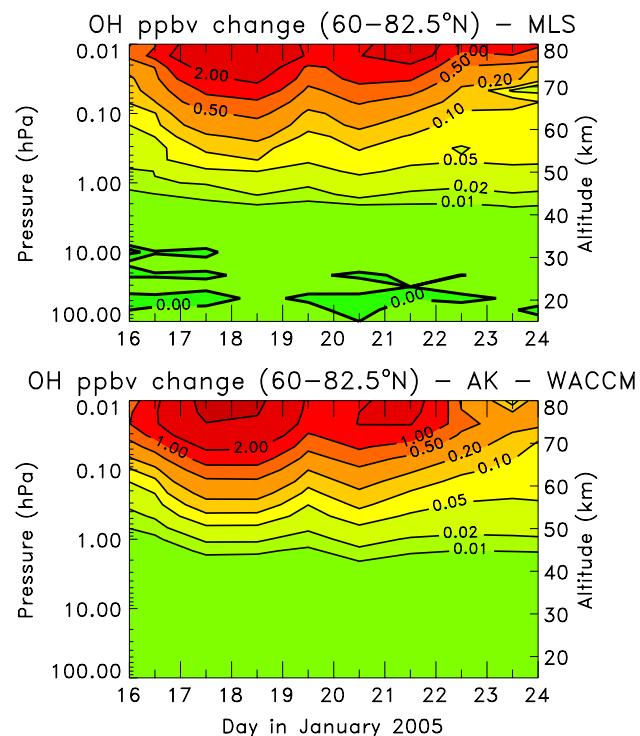


Fig. 5. Daily averaged OH changes from Aura MLS measurements (top) and WACCM3 B average predictions (bottom) for the 60 – 82.5° N band. An average observed (predicted) OH profile for the period 1–14 January 2005 was subtracted from the observed (predicted) OH values for the plotted days (16–23 January 2005). The contour intervals for the OH differences are 0.0, 0.01, 0.02, 0.05, 0.1, 0.2, 0.5, 1, 2, and 5 ppbv. The MLS averaging kernel (AK) was used to sample the WACCM3 results.

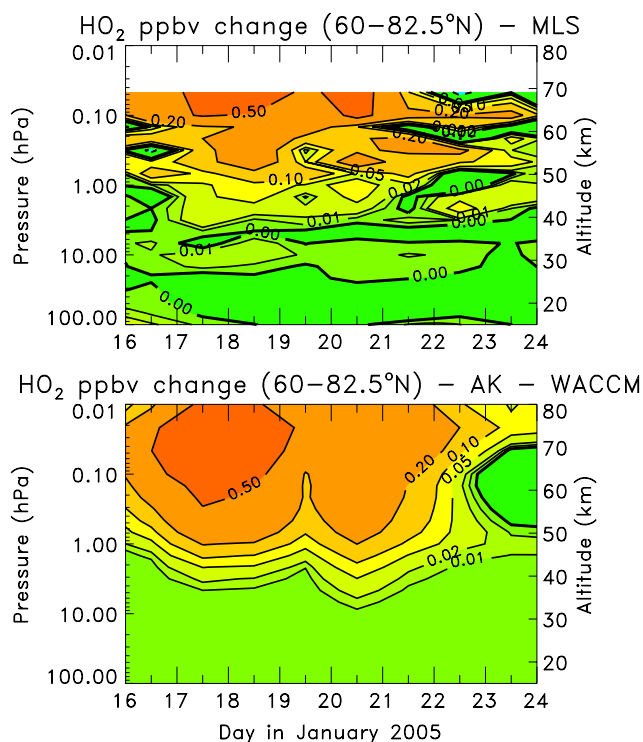


Fig. 6. Daily averaged HO₂ changes from Aura MLS measurements (top) and WACCM3 B average predictions (bottom) for the 60–82.5° N band. An average observed (predicted) HO₂ profile for the period 1–14 January 2005 was subtracted from the observed (predicted) HO₂ values for the plotted days (16–23 January 2005). The contour intervals for the HO₂ differences are –0.1, 0.0, 0.01, 0.02, 0.05, 0.1, 0.2, and 0.5 ppbv. The MLS averaging kernel (AK) was used to sample the WACCM3 results.

5.1.3 Ozone

Besides these two HO_x constituents, MLS also measures ozone. Like Figs. 5 and 6, Fig. 7 was produced by averaging the ozone measurements over the quiet (non-SPE) period 1–14 January 2005 and subtracting this average from the ozone observations or predictions during 16–23 January 2005. As for OH and HO₂, an average of the WACCM3 B realizations sampled with the MLS AK was used for ozone in Fig. 7.

The SPE-produced HO_x constituents are relatively short-lived (~ days) and lead to the destruction of ozone in the uppermost stratosphere and mesosphere. We have found that the WACCM3-predicted ozone change due to the SPEs for the time period plotted is confined to pressures <1 hPa, similar to previous reported studies (e.g., Seppälä et al., 2006; Verronen et al., 2006; Klekociuk et al., 2007). Ozone decreases (>40%) are measured and predicted for the 17–23 January 2005 period at pressures <0.4 hPa. Although there is reasonable agreement between WACCM3 and MLS, the model predictions indicate a slightly deeper penetration of the SPE-caused ozone depletion signal.

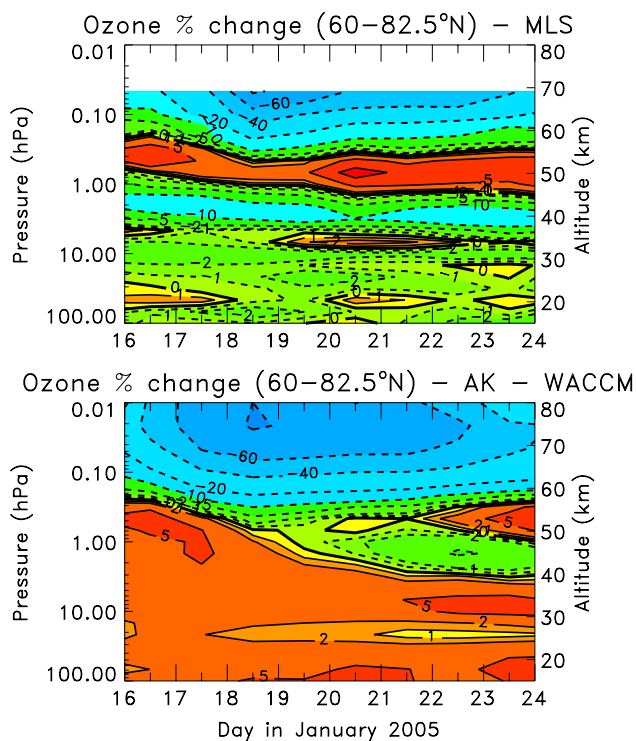


Fig. 7. Daily averaged ozone changes from Aura MLS measurements (top) and WACCM3 B average predictions (bottom) for the 60–82.5° N band. An average observed (predicted) ozone profile for the period 1–14 January 2005 was subtracted from the observed (predicted) ozone values for the plotted days (16–23 January 2005). The contour intervals for the ozone differences are –80, –60, –40, –20, –10, –5, –2, –1, 0, 1, 2, 5, and 10%. The MLS averaging kernel (AK) was used to sample the WACCM3 results.

Based on a similar analysis of the WACCM3 A realizations (not shown), the changes in ozone for pressures >1 hPa in Fig. 7 appear to be caused by seasonal changes at this time of year and are not related to the January 2005 SPEs.

5.1.4 Hydrogen peroxide (H₂O₂)

Envisat MIPAS has recently been shown to have the capability of observing hydrogen peroxide (H₂O₂) (Versick et al., 2009; Versick, 2010) and has provided these measurements in January 2005 during the SPEs. We use here H₂O₂ data (version V4O_H2O2_304) retrieved with the MIPAS level 2 processor developed and operated by the Institute of Meteorology and Climate Research (IMK) in Karlsruhe together with the Instituto de Astrofísica de Andalucía (IAA) in Granada. The main source for H₂O₂ is the HO₂ self-reaction



with a smaller contribution from the three-body reaction



Thus, production of OH and HO₂ by the SPEs leads very rapidly to the production of H₂O₂. Figure 8 (top) shows the polar (60–82.5° N) MIPAS observed 24-h average H₂O₂ for three days (16–18 January 2005) throughout most of the stratosphere and into the lowermost mesosphere. H₂O₂ changes during the three days of the first January 2005 SPE (see Sect. 2) are minor at pressure levels greater than 30 hPa. At pressure levels less than 30 hPa, H₂O₂ is measured to increase during these three days with the largest increases in the lowermost mesosphere (~60 pptv).

Figure 8 (middle) shows the polar (60–82.5° N) WACCM3 predicted 24-h average H₂O₂ for the same three days using an average of the B realizations. Generally, the modeled amounts of H₂O₂ are substantially more than the measured values throughout the plotted domain. H₂O₂ is predicted to increase 180 pptv (~130 pptv to ~310 pptv) in the lowermost mesosphere, about a factor of three larger than observed by MIPAS. Figure 8 (bottom) shows the enhanced H₂O₂ due to the SPEs and is the difference between an average of the A realizations and an average of the B realizations. H₂O₂ is predicted to increase at all pressure levels during these three days as a result of the SPEs. For better direct comparisons, the MIPAS AK was applied to the plotted WACCM3 results.

What is the reason behind the measurement and model H₂O₂ differences? Since the OH and HO₂ predictions are higher than the MLS measurements, it does follow that H₂O₂ would likely be overestimated, given the major production reactions (Eqs. 1 and 2). The major loss of H₂O₂ during daylight is through photolysis



During nighttime the reaction



is the major loss process for H₂O₂. Reaction (4) is especially important in the northern polar latitudes in January, thus is most significant for this study. The HO_x production from SPEs is in the form of OH and H (Solomon et al., 1981). These constituents can very rapidly lead to HO₂ production through



and



The HO_x constituents are primarily lost through reactions



and



or

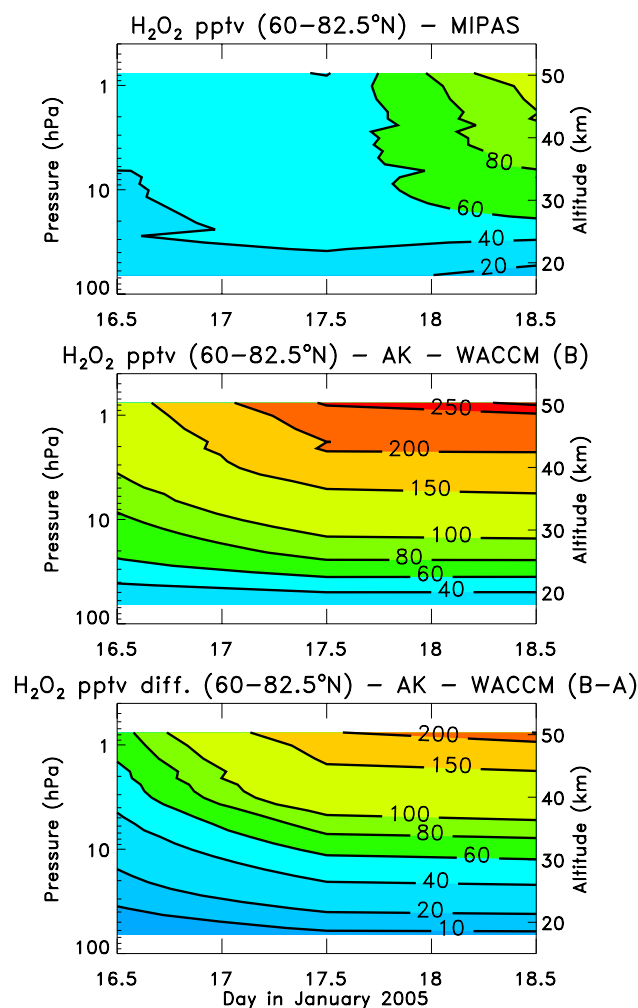


Fig. 8. Daily averaged hydrogen peroxide (H₂O₂): Envisat MIPAS measurements (top) and WACCM3 predictions (middle, bottom) for three days, 16–18 January 2005, in the 60–82.5° N band. The WACCM3 results are from the B average (middle) and a difference between the B average and A average (bottom). The MIPAS averaging kernel (AK) was used to sample the WACCM3 results. The contour intervals are 10, 20, 40, 60, 80, 100, 150, 200, 250, and 300 pptv.

Other reactions, besides Reaction (1) through Reaction (9), are important as well and involve HO_x species with other atmospheric constituents. All the neutral constituent photochemical reaction rates and photodissociation cross sections are taken from Sander et al. (2006). It is unclear which reaction (or reactions) may need to be modified to rectify the differences between MIPAS and WACCM3 H₂O₂. These measurement/model disagreements may be related to the difficulties in simulating OH and HO₂ (e.g., see Canty et al., 2006) and require further study.

5.2 Medium-term influences

SPE-produced NO_x constituents have longer lifetimes than HO_x constituents (e.g., Jackman et al., 2008) and can cause atmospheric changes for several weeks or longer following such events. López-Puertas et al. (2005a) has shown large Envisat MIPAS NO_x enhancements caused by the October–November 2003 SPEs as well as associated ozone depletion over a two and a half week period. The proton flux during the January 2005 SPEs was not quite as significant as the proton flux during the October–November 2003 SPEs, however, the SPE-induced NO_x change did occur in the middle of the NH winter when the impact can be enhanced through a longer lifetime and downward transport (Jackman et al., 2000). We focus on the Northern Hemisphere as any NO_x signal is most likely to last longer in the darker hemisphere (e.g., Jackman et al., 2008). Quantifying the influence of the NO_x produced by the January 2005 SPEs is one of the main objectives of this paper.

5.2.1 Nitrogen dioxide (NO_2)

Envisat MIPAS provided measurements for some days during the month of January 2005. In particular, we show the four-day average (10–13 January 2005) MIPAS NO_2 measurements (IMK/IAA data version V4O_NO2_501) in Fig. 9 (top) before any major SPE disturbance. Although the measured NO_2 amounts are at modest levels (~ 4 – 10 ppbv) in the middle latitudes (40 – 60° N), the observed polar middle mesosphere NO_2 can be quite substantial, reaching peak amounts of about 120 ppbv near 70 km (~ 0.03 hPa) at the highest northern latitudes.

WACCM3 predictions of NO_2 for the same time period are given in Fig. 9 (bottom). The model results do show relatively modest levels (~ 1 – 10 ppbv) in the middle latitudes, fairly similar to MIPAS observations. However, WACCM3 only shows peak values < 15 ppbv near 70 km (~ 0.03 hPa) at the highest northern latitudes, very different from MIPAS measurements. It appears that MIPAS measurements are indicative of a very disturbed mesosphere before the SPEs commence on 16 January. Seppälä et al. (2007) likewise showed high NO_2 mixing ratios (> 30 ppbv) in the Northern Hemisphere polar lower mesosphere in early January 2005, measured by the GOMOS instrument.

We used our WACCM3 simulations to compute the NO_2 change over the 16–23 January 2005 period in Fig. 10. This NO_2 change was computed by subtracting the four-day average (10–13 January 2005) values from the 16–23 January predictions using an average of the B realizations. The results pertain to the average in the latitude band from 70° – 90° N. Nitrogen dioxide enhancements over 30 ppbv are computed in the 60–70 km (0.2–0.03 hPa) altitude region for 18–20 January 2005.

The MIPAS measurements are not shown over the 16–23 January 2005, period due to its limited coverage as the

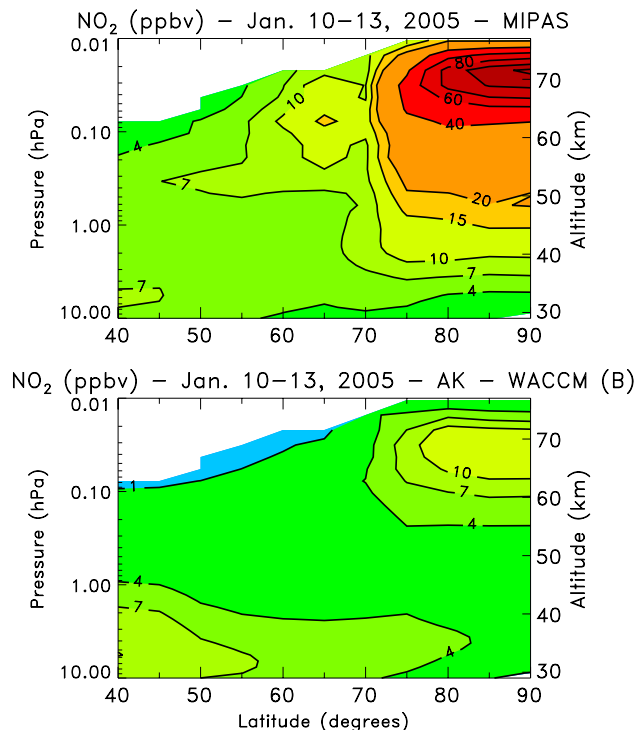


Fig. 9. Envisat MIPAS NO_2 measurements (top) and WACCM3 B average (bottom) for the four-day (10–13 January 2005) average in the Northern Hemisphere. The MIPAS averaging kernel (AK) was used to sample the WACCM3 results. The contour intervals are 1, 4, 7, 10, 15, 20, 40, 60, 80, 100, and 120 ppbv.

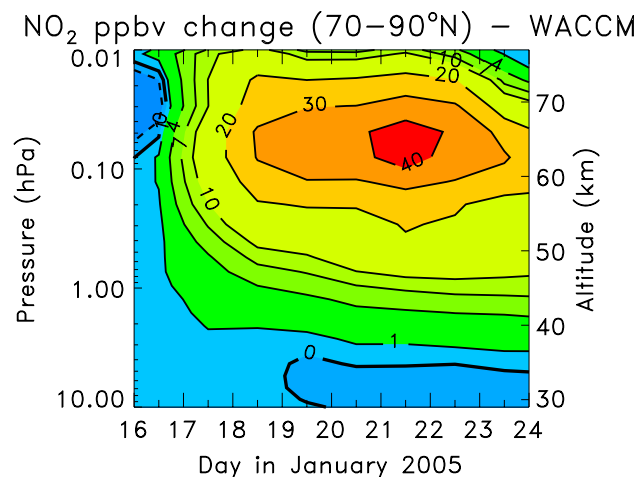


Fig. 10. Daily averaged WACCM3 B average of NO_2 change from the four-day (10–13 January 2005) mean for the 70° – 90° N band. The contour intervals are -1 , 0, 1, 4, 7, 10, 20, 30, and 40 ppbv.

instrument was measuring in its upper troposphere/lower stratosphere mode with an uppermost temperature retrieval of just 50 km. The temperature above 50 km was not measured and the assumed temperature was too high in this

region and greatly impacted the NO_2 . The TIMED Sounding of the Atmosphere using Broadband Emission Radiometry (SABER) instrument took measurements during this time period and showed that the assumed MIPAS temperatures were about 10–12 K too warm in the 50–60 km region. Some preliminary computations with temperatures more similar to SABER (i.e., decreased by 10–12 K) have resulted in enhanced MIPAS NO_2 values during the first SPE period (16–18 January 2005) of about 30 ppbv over the 10–13 January levels. Thus, even though the MIPAS NO_2 observations before the SPEs are very different, the deduced MIPAS NO_2 increases as a result of the first SPE are fairly similar to the WACCM3 predictions.

5.2.2 Nitric acid (HNO_3)

The SPE-caused impact on HNO_3 has been discussed before in relation to the October–November 2003 SPEs (Orsolini et al., 2005; López-Puertas et al., 2005b; Jackman et al., 2008; Verronen et al., 2008). Jackman et al. (2008) showed Envisat MIPAS measured HNO_3 enhancements of over 2 ppbv near 1 hPa as a result of the late October 2003 SPE, however, the WACCM3 simulations predicted a smaller maximum enhancement of 0.8 ppbv near 1 hPa.

Klekociuk et al. (2007) demonstrated HNO_3 enhancements in Aura MLS measurements as well as global model computations as a result of the January 2005 SPEs. We have analyzed MLS HNO_3 measurements in a similar manner to Klekociuk et al. (2007) and show the results in Fig. 11 (top). Here, an average MLS HNO_3 for the period 1–14 January 2005, before the first SPE, was subtracted from the MLS HNO_3 for 16–29 January 2005 in the 60–82.5° N band. Envisat MIPAS HNO_3 measurements are also available in January 2005, but only for a limited number of days (i.e., 10–13, 16–18, 27–28 January). Because of this limited dataset, the four-day average of the MIPAS measurements before the first SPE (i.e., 10–13 January 2005) was subtracted from the 16–18 and 27–28 January 2005 values (IMK/IAA data version V40_HNO3_201); this difference is given in Fig. 11 (middle). The WACCM3 results are presented in Fig. 11 (bottom), where a HNO_3 average of the B realizations for the period 1–14 January 2005 before the first SPE was subtracted from the modeled HNO_3 for 16–29 January 2005 in the 60°–82.5° N band.

The MLS HNO_3 measurements indicated two enhanced regions (3–9 and 20–40 hPa) during the 16–25 January 2005 period (also, see Klekociuk et al., 2007) with a region of decreased HNO_3 in between. Also, MLS shows decreased HNO_3 between 40 and 100 hPa. The MIPAS HNO_3 observations show similarities to the MLS data on 27–28 January for pressure levels less than 9 hPa and more than 15 hPa, however, there is not an indication of the region of decreased HNO_3 between 9 and 15 hPa. The WACCM3 predicted HNO_3 change shows decreases between about 4 and 50 hPa during 16–23 January 2005, with a slight increase at pres-

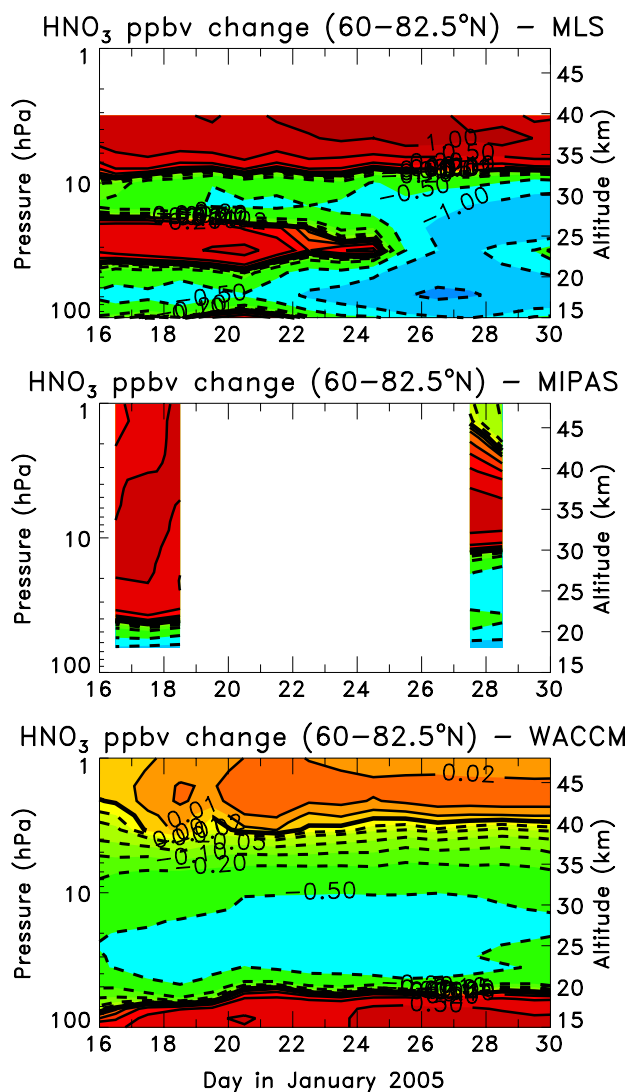


Fig. 11. Daily averaged nitric acid (HNO_3) change: Aura MLS measurements (top), Envisat MIPAS measurements (middle), and WACCM3 B average (bottom) for 16–29 January 2005 in the 60°–82.5° N band. A mean HNO_3 for the period 1–14 January 2005 was subtracted from the Aura MLS observed and WACCM3 B average predicted values for the plotted days. Envisat MIPAS measurements were only available for 10–13 January 2005, and the average of these four days was subtracted from the 16–18 and 27–28 January 2005 values. The contour intervals are $-2, -1, -0.5, -0.2, -0.1, -0.05, -0.02, -0.01, 0, 0.01, 0.02, 0.05, 0.1, 0.2, 0.5,$ and 1 ppbv.

ures less than 4 hPa. An average of the WACCM3 A realizations, which is not shown, gives nearly the same results as those predicted from an average of the WACCM3 B realizations, the only difference being the small SPE-caused 0.02–0.04 ppbv enhanced HNO_3 region near 3 hPa over most of the time period. Since WACCM3 results were compared with both MLS and MIPAS observations, neither instrument array of AKs were used to process the WACCM3 output. These

model/measurement comparisons leave us with the dilemma found in Jackman et al. (2008) whereby large increases in observed HNO_3 temporally connected to SPEs could not be properly simulated.

The creation of HNO_3 through the ion-ion recombination between H^+ and NO_3^- cluster ions was simulated during another solar proton event period, the Halloween storm episode in October–November 2003, with the use of the Sodankylä Ion and Neutral Chemistry model in Verronen et al. (2008). They showed that the HNO_3 production above 35 km as a result of those large events could account for the extra HNO_3 observed by MIPAS in October/November 2003. It is likely that this ion chemistry, currently not included in WACCM3, could also explain the MLS and MIPAS observed additional 0.5–1 ppbv HNO_3 above 35 km (pressures <7 hPa) seen in Fig. 11.

5.2.3 Nitrogen oxides, NO_x ($\text{NO} + \text{NO}_2$)

ACE-FTS (hereinafter referred to as ACE) (Bernath et al., 2005) provided measurements during all of the SPE period. ACE measured both NO and NO_2 (e.g., see Rinsland et al., 2005), and thus supplied NO_x ($\text{NO} + \text{NO}_2$) measurements at fairly high northern latitudes for 1–31 January 2005. These ACE observations are given in Fig. 12a and were taken in the latitude range from ~ 57 – 66°N (see Fig. 12, top). Large amounts of NO_x are observed at pressures <0.01 hPa with evidence of some downward transport over this time period, especially in the latter half of the month. We focus on pressures >0.01 hPa, where there is an indication of a large perturbation around 16 January. After that date the contour levels 20, 50, 100, and 200 ppbv show substantially more NO_x measured in the pressure range 0.02 to about 0.4 hPa (~ 55 –75 km).

The ACE measurements (Fig. 12a) are compared with similar plots from our WACCM3 simulations in Fig. 12b, c. The WACCM3 results are taken from the model predictions for the 60 – 66°N latitude bins, approximately the latitude range for the ACE Northern Hemisphere measurements after 6 January 2005. There are no AKs for the ACE instrument because optimal estimation is not used in the ACE retrievals, thus the unprocessed WACCM3 output is used for these comparisons. Figure 12c shows WACCM3 NO_x predictions from an average of the A realizations. This plot does not indicate much of a change in NO_x over the month. In fact, the predicted NO_x in the pressure range 0.02 to 0.4 hPa after 16 January appears to show a slight decrease at most levels. Figure 12b shows WACCM3 NO_x predictions from an average of the B realizations. These model predictions show a dramatic change after 16 January with large NO_x increases due to the SPEs, as indicated by changes in the slopes of contour levels 10, 20, 50, and 100 ppbv.

The NO_x variations over the three month time period (1 January–31 March 2005) are given in Fig. 13. Again, ACE measurements are shown in the top plot. There is a change in

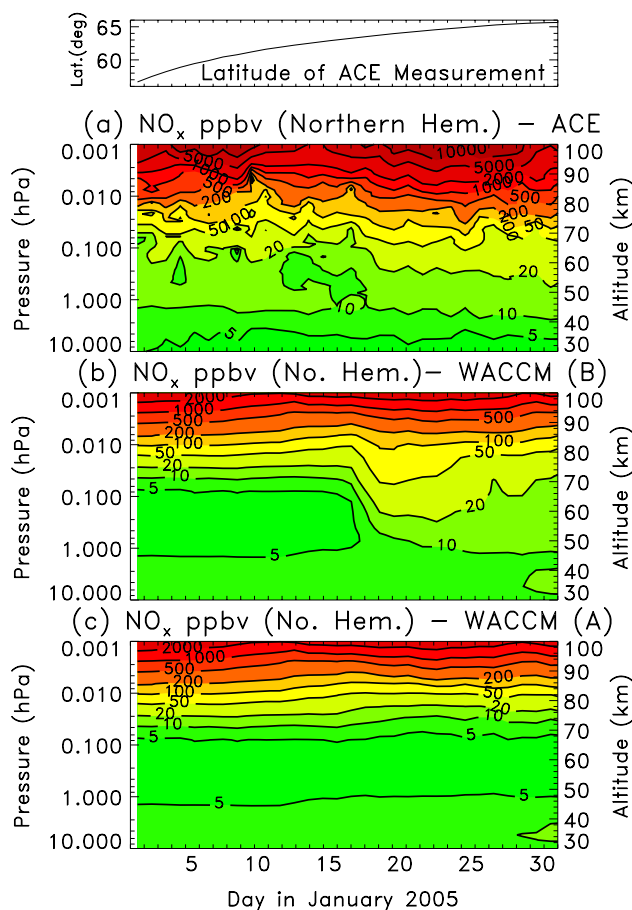


Fig. 12. Daily averaged NO_x measurements (a) and predictions (b, c) for 1–31 January 2005 in the high latitude Northern Hemisphere (see Sect. 5.2.3). The ACE NO_x measurements are given in (a). The WACCM3 NO_x predictions are from an average of the B realizations (b) and the A realizations (c). The contour intervals for NO_x are 1, 2, 5, 10, 20, 50, 100, 200, 500, 1000, 2000, 5000, and 10 000 ppbv. The latitudes of ACE measurements are given in the top plot.

the slopes of the NO_x contours after Day of Year (DoY) 32, when NO_x amounts tend to decrease with time at virtually all levels above ~ 1 hPa. ACE observes at latitudes greater than 60°N up through DoY 83 (24 March), thus this NO_x change is probably related more to a seasonal effect, not related to the SPEs, than to the variation in ACE measurement latitudes during the season. After DoY 83, the latitude observed by ACE varies rapidly from 60°N to 41°N by DoY 90. These rapid changes in observed latitude help to explain the fast decrease of observed NO_x in the last week plotted in Fig. 13 (top). Downward transport of thermospheric NO_x in the winter and early spring, not related to the SPEs, is much larger at polar latitudes than middle latitudes (e.g., Randall et al., 2005, 2006).

MIPAS also measured NO_x for 16 days (e.g., DoYs 27–28, 38, 44–46, 48–49, 52–53, 61–62, 67–68, and 80–81) in this

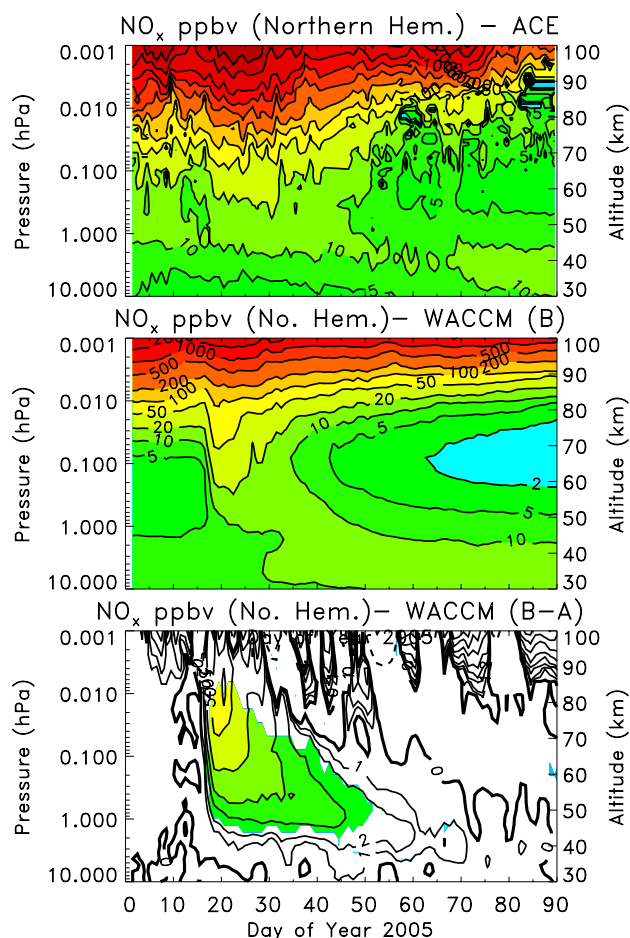


Fig. 13. Daily averaged SCISAT-1 ACE measurements (top) and WACCM3 predictions (middle, bottom) for NO_x during the first 90 days of 2005 (1 January–31 March) for the high latitude Northern Hemisphere. The WACCM3 NO_x predictions (middle) are from an average of the B realizations and the WACCM3 NO_x predictions (bottom) show the NO_x enhancement due to the SPEs (an average of the B realizations minus an average of the A realizations). The colored regions indicate 95 % statistical significance with the use of Student's t test. The contour intervals are 1, 2, 5, 10, 20, 50, 100, 200, 500, 1000, 2000, 5000, and 10 000 ppbv.

period over a limited altitude range on most days. We have found that, generally, MIPAS observations are in reasonable agreement with ACE (not shown).

Figure 13 (middle) shows WACCM3 NO_x predictions (60–66° N) from an average of the B simulations (SPEs-only), essentially an extension of Fig. 12b for another 59 days. There are many similarities between these model computations and the ACE measurements. The change in slope of the contour levels indicating a decrease in NO_x at virtually all levels above ~ 1 hPa occurs in the model simulations at about DoY 25 (rather than the DoY 32 in the ACE measurements), however, qualitatively the model results and ACE measurements are in reasonable agreement.

We are able to compute the quantitative NO_x enhancement due to the SPEs by subtracting an average of the A realizations from the average of the B realizations. These results are given in Fig. 13 (bottom), where the colored regions indicate 95 % statistical significance with the use of Student's t test. The SPEs caused NO_x increases > 50 ppbv in the middle to upper mesosphere. These NO_x enhancements diminished over time to be less than 5 ppbv and no longer statistically significant by DoY 50. Thus, the SPE-caused NO_x increases from the January 2005 SPEs lasted for about one month past the beginning of the events.

5.2.4 Ozone and temperature

We computed the ozone change due to SPEs over the 1 January–31 March 2005 period by comparing the average of the B realizations relative to an average of the A realizations. The large ozone decreases shown in Fig. 7 extended another two days (through DoY 25), however, statistically significant (to 95 %) NH polar mesospheric ozone loss computed with Student's t test was evident only from DoY 17–23. Ozone depletion less than 5 % due to the SPEs was calculated for a couple of weeks past the end of January. These results are consistent with the SPE-induced short-lived HO_x enhancements causing most of the mesospheric ozone loss.

We also computed the temperature change due to SPEs over the 1 January–31 March 2005 period by comparing the average of the B realizations relative to an average of the A realizations. These computed temperature changes were less than 3 K during the time period of the large computed ozone losses (DoY 17–23) and were not statistically significant. Such small temperature changes are consistent with Jackman et al. (2007) and are not surprising in the limited sunlit polar region (NH) where less ozone heating occurs.

6 Influences of the 20 January 2005 GLE

As discussed previously (Sects. 1 and 2), a very large GLE occurred on 20 January 2005, during the SPE period. Although the flux of very energetic protons was extremely high, the duration of this intense flux was fairly short (less than about 8 h for the highest energy protons, see NOAA GOES-11 data). The most substantial increase in the high energy protons lasted only about 90 m (Simnett and Roelof, 2005). Also, these very high energy protons primarily impacted the middle to lower stratosphere (10–100 hPa, see Fig. 2), thus the influence on this lower region of the atmosphere is diluted by the increased number density of molecules (compared to the mesosphere). A daily averaged GLE ionization rate is used for consistency with the other WACCM3 computations.

Since the NO_x family rapidly converts in the stratosphere to other constituents in the odd nitrogen group ($\text{NO}_y = \text{N}(^4\text{S}) + \text{N}(^2\text{D}) + \text{NO} + \text{NO}_2 + \text{NO}_3 + 2\text{N}_2\text{O}_5 + \text{HNO}_3 + \text{HO}_2\text{NO}_2 + \text{ClONO}_2 + \text{BrONO}_2$), it is appropriate

to concentrate on the NO_y impact due to the GLE. We have computed the percentage change of NO_y at polar northern latitudes ($60\text{--}90^\circ\text{N}$) over the 19–23 January 2005 period by subtracting an average of the C realizations from an average of the B realizations and present these results in Fig. 14. As a result of the GLE, odd nitrogen is calculated to be enhanced by a maximum of about 0.09%, a very small increase. Ozone changes appear to be connected to these NO_y enhancements and show a maximum of about a 0.007% decrease. Although the computed HO_x changes due to the GLE are larger ($>20\%$ in the 20–100 hPa range), this seemingly significant impact is mainly due to the small amount of ambient HO_x in the polar very low sun conditions at this time of year. Ambient HO_x values in the $60\text{--}90^\circ\text{N}$ region range from 0.002–0.3 pptv at 100 hPa to 1.2–1.9 pptv at 20 hPa. The computed HO_x enhancement is short-lived and is essentially gone within 48 h due to the short lifetime of the HO_x constituents.

As an aside, the polar southern latitudes ($60\text{--}90^\circ\text{S}$) were also impacted in a minor way due to this GLE. NO_y was increased in the lower stratosphere by a maximum of 0.18% and ozone was decreased by a maximum of 0.05% when WACCM3 B results were compared with C results. The southern polar HO_x was enhanced by a maximum of 2%, but this enhancement was gone within 24 h.

These WACCM3 simulations indicate that inclusion of the GLE on 20 January leads to very small atmospheric constituent perturbations.

7 Conclusions

The January 2005 SPEs caused large enhancements in the northern polar mesospheric HO_x and NO_x constituents, which were both observed and modeled. Aura MLS observations indicated large mesospheric increases in OH (up to 4 ppbv) and HO_2 (>0.5 ppbv) as a result of the SPEs during the time period 16–21 January in the $60\text{--}85^\circ\text{N}$ latitude band. The WACCM3 simulations showed quantitatively similar, although somewhat larger enhancements in OH and HO_2 . These large HO_x enhancements led to considerable MLS-measured and predicted ozone decreases of greater than 40% throughout most of the northern polar mesosphere during the SPE period. MIPAS measured H_2O_2 enhancements through the stratosphere into the lower mesosphere (reaching ~ 60 pptv) from 16 January to 18 January. WACCM3 also predicted H_2O_2 increases over the same period, however, these predictions were about a factor of three larger than observed.

Nitric acid measured by both MLS and MIPAS increased in the upper stratosphere during 16–23 January when compared with 1–14 January 2005, however, WACCM3 predictions indicated only minor enhancements in the same time period and altitude range. WACCM3 currently lacks ion chemical reactions responsible for the SPE-caused cre-

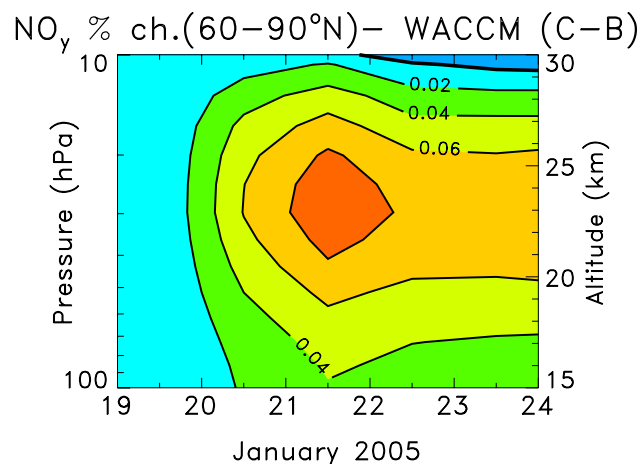


Fig. 14. Daily averaged WACCM3 prediction of the polar Northern Hemisphere ($60\text{--}90^\circ\text{N}$) NO_y percentage enhancement due to the GLE (the average of the C realizations minus the average of the B realizations). The contour intervals are 0.0, 0.02, 0.04, 0.06, and 0.08%.

ation of HNO_3 (Verronen et al., 2008). MIPAS observations showed large enhancements of polar middle mesospheric NO_2 before the SPEs, which were likely the result of NO_x winter descent from higher altitudes (also, see GOMOS measurements in Seppälä et al., 2007). However during the SPEs, WACCM3 simulated a mesospheric NO_2 enhancement of greater than 30 ppbv in the $60\text{--}70$ km ($0.2\text{--}0.03$ hPa) altitude region for 18–20 January 2005 in the polar Northern Hemisphere, which is in reasonable agreement with inferred MIPAS NO_2 increases over the same altitude region. WACCM3 predictions are in reasonable agreement with SCISAT-1 ACE measurements of NO_x enhancements for the Northern Hemisphere. The observed and predicted enhancements are considerable for the mesosphere and led to statistically significant NO_x increases in polar northern latitudes for about a month past the SPEs.

We found that protons of energies 300 to 20 000 MeV, associated with the GLE on 20 January, led to enhanced stratospheric NO_y of less than 0.1% and ozone decreases of less than 0.01% in the northern polar latitudes. Thus, protons with energies less than 300 MeV had a much larger impact on the middle atmosphere in January 2005 than higher energy protons from the GLE.

Acknowledgements. We thank NASA Headquarters Living With a Star Targeted Research and Technology Program and the Aura Science Team Program for support during the time that this manuscript was written. CER was supported by NASA LWS grants NNX08AU44G and NNX06AC05G. We thank Nathaniel Livesey, Shuhui Wang, and Herbert Pickett of the Aura MLS Team for help in utilizing the MLS measurements and application of the MLS averaging kernels to WACCM3 output. We thank Gordon J. Labow (Science Systems and Applications, Inc.) for help with plotting Figs. 3 and 4. We thank the NOAA GOES team for providing the

solar proton flux data over the Internet. The National Center for Atmospheric Research is sponsored by the National Science Foundation. WACCM3 results presented in this paper were generated using NASA's Columbia supercomputer housed at the NASA Ames Research Center. The ACE mission is supported primarily by the Canadian Space Agency. Some support was also provided by the UK Natural Environment Research Council, NERC. MIPAS work presented in this paper was funded by the project MANOXUVA within the DFG priority project 1176 CAWSES. The IAA team was supported by the Spanish MICINN under project AYA2008-03498/ESP and EC FEDER funds. MIPAS level-1b data have been provided by ESA.

Edited by: A. J. G. Baumgaertner

References

- Bernath, P. F., McElroy, C. T., Abrams, M. C., Boone, C. D., Butler, M., Camy-Peyret, C., Carleer, M., Clerbaux, C., Coheur, P. F., Colin, R., DeCola, P., DeMazière, M., Drummond, J. R., Dufour, D., Evans, W. F. J., Fast, H., Fussen, D., Gilbert, K., Jennings, D. E., Llewellyn, E. J., Lowe, R. P., Mahieu, E., McConnell, J. C., McHugh, M., McLeod, S. D., Michaud, R., Midwinter, C., Nassar, R., Nichitiu, F., Nowlan, C., Rinsland, C. P., Rochon, Y. J., Rowlands, N., Semeniuk, K., Simon, P., Skelton, R., Sloan, J. J., Soucy, M.-A., Strong, K., Tremblay, P., Turnbull, D., Walker, K. A., Walkty, I., Wardle, D. A., Wehrle, V., Zander, R., and Zou, J.: Atmospheric Chemistry Experiment (ACE): mission overview, *Geophys. Res. Lett.*, 32, L15S01, doi:10.1029/2005GL022386, 2005.
- Canty, T., Pickett, H. M., Salawitch, R. J., Jucks, K. W., Traub, W. A., and Waters, J. W.: Stratospheric and mesospheric HO_x: results from Aura MLS and FIRS-2, *Geophys. Res. Lett.*, 33, L12802, doi:10.1029/2006GL025964, 2006.
- Damiani, A., Storini, M., Laurenza, M., and Rafanelli, C.: Solar particle effects on minor components of the Polar atmosphere, *Ann. Geophys.*, 26, 361–370, doi:10.5194/angeo-26-361-2008, 2008.
- Damiani, A., Diego, P., Laurenza, M., Storini, M., and Rafanelli, C.: Ozone variability related to SEP events occurring during solar cycle no. 23, *Adv. Space Res.*, 43, 28–40, 2009.
- Damiani, A., Storini, M., Rafanelli, C., and Diego, P.: The hydroxyl radical as an indicator of SEP fluxes in the high-latitude terrestrial atmosphere, *Adv. Space Res.*, 46, 1225–1235, 2010.
- Forkman, P., Eriksson, P., Winnberg, A., Garcia, R. R., and Kinnison, D.: Longest continuous ground-based measurements of mesospheric CO, *Geophys. Res. Lett.*, 30, 1532, doi:10.1029/2003GL016931, 2003.
- Garcia, R. R., Marsh, D. R., Kinnison, D. E., Boville, B. A., and Sassi, F.: Simulation of secular trends in the middle atmosphere, 1950–2003, *J. Geophys. Res.*, 112, D09301, doi:10.1029/2006JD007485, 2007.
- Gopalswamy, N., Xie, H., Yashiro, S., and Usoskin, I.: Coronal mass ejections and ground level enhancements, 29th International Cosmic Ray Conference Pune, India, 1, 101–104, 3–10 August 2005.
- Jackman, C. H. and McPeters, R. D.: The response of ozone to solar proton events during solar cycle 21: a theoretical interpretation, *J. Geophys. Res.*, 90, 7955–7966, 1985.
- Jackman, C. H., Frederick, J. E., and Stolarski, R. S.: Production of odd nitrogen in the stratosphere and mesosphere: an intercomparison of source strengths, *J. Geophys. Res.*, 85, 7495–7505, 1980.
- Jackman, C. H., Fleming, E. L., and Vitt, F. M.: Influence of extremely large solar proton events in a changing stratosphere, *J. Geophys. Res.*, 105, 11659–11670, 2000.
- Jackman, C. H., McPeters, R. D., Labow, G. J., Fleming, E. L., Praderas, C. J., and Russell, J. M.: Northern Hemisphere atmospheric effects due to the July 2000 solar proton event, *Geophys. Res. Lett.*, 28, 2883–2886, 2001.
- Jackman, C. H., DeLand, M. T., Labow, G. J., Fleming, E. L., Weisenstein, D. K., Ko, M. K. W., Sinnhuber, M., and Russell, J. M.: Neutral atmospheric influences of the solar proton events in October–November 2003, *J. Geophys. Res.*, 110, A09S27, doi:10.1029/2004JA010888, 2005.
- Jackman, C. H., Roble, R. G., and Fleming, E. L.: Mesospheric dynamical changes induced by the solar proton events in October–November 2003, *Geophys. Res. Lett.*, 34, L04812, doi:10.1029/2006GL028328, 2007.
- Jackman, C. H., Marsh, D. R., Vitt, F. M., Garcia, R. R., Fleming, E. L., Labow, G. J., Randall, C. E., López-Puertas, M., Funke, B., von Clarmann, T., and Stiller, G. P.: Short- and medium-term atmospheric constituent effects of very large solar proton events, *Atmos. Chem. Phys.*, 8, 765–785, doi:10.5194/acp-8-765-2008, 2008.
- Jackman, C. H., Marsh, D. R., Vitt, F. M., Garcia, R. R., Randall, C. E., Fleming, E. L., and Frith, S. M.: Long-term middle atmospheric influence of very large solar proton events, *J. Geophys. Res.*, 114, D11304, doi:10.1029/2008JD011415, 2009.
- Kinnison, D. E., Brasseur, G. P., Walters, S., Garcia, R. R., Marsh, D. R., Sassi, F., Harvey, V. L., Randall, C. E., Emmons, L., Lamarque, J. F., Hess, P., Orlando, J. J., Tie, X. X., Randel, W., Pan, L. L., Gettelman, A., Granier, C., Diehl, T., Niemeier, U., and Simmons, A. J.: Sensitivity of chemical tracers to meteorological parameters in the MOZART-3 chemical transport model, *J. Geophys. Res.*, 112, D20302, doi:10.1029/2006JD007879, 2007.
- Klekociuk, A. R., Bombardieri, D. J., Duldig, M. L., and Michael, K. J.: Atmospheric chemistry effects of the 20 January 2005 solar proton event, *Adv. Geosci.*, 14, Solar Terrestrial, 305–319, 2007.
- López-Puertas, M., Funke, B., Gil-López, S., von Clarmann, T., Stiller, G. P., Höpfner, M., Kellmann, S., Fischer, H., and Jackman, C. H.: Observation of NO_x enhancement and ozone depletion in the Northern and Southern Hemispheres after the October–November 2003 solar proton events, *J. Geophys. Res.*, 110, A09S43, doi:10.1029/2005JA011050, 2005a.
- López-Puertas, M., Funke, B., Gil-López, S., von Clarmann, T., Stiller, G. P., Höpfner, M., Kellmann, S., Mengistu Tsidu, G., Fischer, H., and Jackman, C. H.: HNO₃, N₂O₅, and ClONO₂ enhancements after the October–November 2003 solar proton events, *J. Geophys. Res.*, 110, A09S44, doi:10.1029/2005JA011051, 2005b.
- Marsh, D. R., Garcia, R. R., Kinnison, D. E., Boville, B. A., Sassi, F., Solomon, S. C., and Matthes, K.: Modeling the whole atmosphere response to solar cycle changes in radiative and geomagnetic forcing, *J. Geophys. Res.*, 112, D23306,

- doi:10.1029/2006JD008306, 2007.
- McPeters, R. D., Jackman, C. H., and Stassinopoulos, E. G.: Observations of ozone depletion associated with solar proton events, *J. Geophys. Res.*, 86, 12071–12081, 1981.
- Orsolini, Y. J., Manney, G. L., Santee, M. L., and Randall, C. E.: An upper stratospheric layer of enhanced HNO₃ following exceptional solar storms, *Geophys. Res. Lett.*, 32, L12S01, doi:10.1029/2004GL021588, 2005.
- Pickett, H. M., Drouin, B. J., Canty, T., Salawitch, R. J., Fuller, R. A., Perun, V. S., Livesey, N. J., Waters, J. W., Stachnik, R. A., Sander, S. P., Traub, W. A., Jucks, K. W., and Minschwaner, K.: Validation of Aura Microwave Limb Sounder OH and HO₂ measurements, *J. Geophys. Res.* 113, D16S30, doi:10.1029/2007JD008775, 2008.
- Porter, H. S., Jackman, C. H., and Green, A. E. S.: Efficiencies for production of atomic nitrogen and oxygen by relativistic proton impact in air, *J. Chem. Phys.*, 65, 154–167, 1976.
- Randall, C. E., Harvey, V. L., Manney, G. L., Orsolini, Y., Co-drescu, M., Sioris, C., Brohede, S., Haley, C. S., Gordley, L. L., Zawodny, J. M., and Russell, J. M.: Stratospheric effects of energetic particle precipitation in 2003–2004, *Geophys. Res. Lett.*, 32, L05802, doi:10.1029/2004GL022003, 2005.
- Randall, C. E., Harvey, V. L., Singleton, C. S., Bernath, P. F., Boone, C. D., and Kozyra, J. U.: Enhanced NO_x in 2006 linked to strong upper stratospheric Arctic vortex, *Geophys. Res. Lett.*, 33, L18811, doi:10.1029/2006GL027160, 2006.
- Richter, J. H. and Garcia, R. R.: On the forcing of the Mesospheric Semi-Annual Oscillation in the Whole Atmosphere Community Climate Model, *Geophys. Res. Lett.*, 33, L01806, doi:10.1029/2005GL024378, 2006.
- Rinsland, C. P., Boone, C., Nassar, R., Walker, K., Bernath, P., McConnell, J. C., and Chiou, L.: Atmospheric Chemistry Experiment (ACE) Arctic stratospheric measurements of NO_x during February and March 2004: Impact of intense solar flares, *Geophys. Res. Lett.*, 32, L16S05, doi:10.1029/2005GL022425, 2005.
- Sassi, F., Garcia, R. R., Boville, B. A., and Liu, H.: On temperature inversions and the mesospheric surf zone, *J. Geophys. Res.*, 107, 4380, doi:10.1029/2001JD001525, 2002.
- Sassi, F., Kinnison, D., Boville, B. A., Garcia, R. R., and Roble, R.: Effect of El Niño-Southern oscillation on the dynamical, thermal, and chemical structure of the middle atmosphere, *J. Geophys. Res.*, 109, D17108, doi:10.1029/2003JD004434, 2004.
- Seppälä, A., Verronen, P. T., Sofieva, V. F., Tamminen, J., Kyrölä, E., Rodger, C. J., and Clilverd, M. A.: Destruction of the tertiary ozone maximum during a solar proton event, *Geophys. Res. Lett.*, 33, L07804, doi:10.1029/2005GL025571, 2006.
- Seppälä, A., Verronen, P. T., Clilverd, M. A., Randall, C. E., Tamminen, J., Sofieva, V., Backman, L., and Kyrölä, E.: Arctic and Antarctic polar winter NO_x and energetic particle precipitation in 2002–2006, *Geophys. Res. Lett.*, 34, L12810, doi:10.1029/2007GL029733, 2007.
- Simnett, G. M., and Roelof, E., C.: Timing of the relativistic proton acceleration responsible for the GLE on 20 January, 2005, 29th International Cosmic Ray Conference Pune, India, 1, 233–236, 3–10 August 2005.
- Solomon, S., Rusch, D. W., Gerard, J.-C., Reid, G. C., and Crutzen, P. J.: The effect of particle precipitation events on the neutral and ion chemistry of the middle atmosphere. 2. Odd hydrogen, *Planet. Space Sci.*, 29, 885–892, 1981.
- Solomon, S., Reid, G. C., Rusch, D. W., and Thomas, R. J.: Mesospheric ozone depletion during the solar proton event of July 13, 1982, Part II. Comparison between theory and measurements, *Geophys. Res. Lett.*, 10, 257–260, 1983.
- Tylka, A. J. and Dietrich, W. F.: A new and comprehensive analysis of proton spectra in ground-level enhanced (GLE) solar particle events, in: Proceedings of the 31st ICRC, Lodz, 7–15 July 2009.
- Usoskin, I. G., Tylka, A. J., and Kovaltsov, G. A.: Ionization effect of strong particle events: low-middle atmosphere, in: Proceedings of the 31st ICRC, Lodz, 7–15 July 2009.
- Usoskin, I. G., Kovaltsov, G. A., Mironova, I. A., Tylka, A. J., and Dietrich, W. F.: Ionization effect of solar particle GLE events in low and middle atmosphere, *Atmos. Chem. Phys.*, 11, 1979–1988, doi:10.5194/acp-11-1979-2011, 2011.
- Verronen, P. T., Seppälä, A., Kyrola, E., Tamminen, J., Pickett, H. M., and Turunen, E.: Production of odd hydrogen in the mesosphere during the January 2005 solar proton event, *Geophys. Res. Lett.*, 33, L24811, doi:10.1029/2006GL028115, 2006.
- Verronen, P. T., Rodger, C. J., Clilverd, M. A., Pickett, H. M., and Turunen, E.: Latitudinal extent of the January 2005 solar proton event in the Northern Hemisphere from satellite observations of hydroxyl, *Ann. Geophys.*, 25, 2203–2215, doi:10.5194/angeo-25-2203-2007, 2007.
- Verronen, P. T., Funke, B., López-Puertas, M., Stiller, G. P., von Clarmann, T., Glatthor, N., Enell, C.-F., Turunen, E., and Tamminen, J.: About the increase of HNO₃ in the stratopause region during the Halloween 2003 solar proton event, *Geophys. Res. Lett.*, 35, L20809, doi:10.1029/2008GL035312, 2008.
- Versick, S.: Ableitung von H₂O₂ aus MIPAS/ENVISAT-Beobachtungen und Untersuchung der Wirkung von energetischen Teilchen auf den chemischen Zustand der mittleren Atmosphäre, Ph.D. Dissertation (in German), Karlsruher Institute für Technologie, Karlsruhe, Germany, 2010.
- Versick, S., Stiller, G., Glatthor, N., Reddmann, T., Ruhnke, R., von Clarmann, T., Höpfner, M., Kiefer, M., Linden, A., Kellmann, S., and Grabowski, U.: MIPAS-observations and model results for H₂O₂ with focus on the SPEs 2003 and 2005, poster presented at the 2nd International High Energy Particle Precipitation in the Atmosphere (HEPPA) Workshop, Boulder, CO, 6–8 October, 2009.